OURNAL OF SOLID STATE CHEMISTRY 6, 493–501 (1973)

xploring the $A^+B^{5+}O_3$ Compounds*

JOHN B. GOODENOUGH AND JAMES A. KAFALAS

Lincoln Laboratory, Massachusetts Institute of Technology, Lexington, Massachusetts 02173

Received May 31, 1972

The several structures exhibited by $A^+B^{5+}O_3$ compositions having B = Nb, Ta, Sb or Bi are summarized. New phases, prepared either by high-pressure techniques or by ion exchange, are included. Their stability is interpreted qualitatively in terms of four principal factors: relative ionic sizes, Madelung energy, polarizability of A-cation cores, and the covalent contribution to the B–O bonds. This latter contribution inhibits the formation of 180° Sb–O–Sb or Bi–O–Bi bond angles, whereas electrostatic forces inhibit the formation of Sb–Sb or Bi–Bi pairs in octahedral sites sharing a common face. A strong π-bond contribution to the B–O covalency weakens both these constraints for Nb^{5+} and Ta^{5+} ions. A criterion for ferroelectric distortions of the cubic–perovskite phase is presented, and evidence for polarizability of the $3d^{10}$ and $4d^{10}$ cores of Cu^+ and Ag^+ ions is cited.

I. Introduction

Given B cations that are stable in octahedral sites and also atomic radii $r_A > r_B$, the structure of a composition ABO_3 depends upon relative A-ion size, the electrostatic Madelung energy, the character of the B–O and A–O bonds, and any B–B bonding via partially filled d shells at the B cations. The purpose of this study is to explore the influence of the first three of these factors on the relative stabilities of competitive structures for the $A^+B^{5+}O_3$ compositions containing octahedral-site B^{5+} cations. In order to eliminate complications due to B–B bonding, the discussion is limited to octahedral-site B^{5+} ions containing no outer d electrons. However, the transition metal cations Nb^{5+} and Ta^{5+} are compared with the pnicogen cations Sb^{5+} and Bi^{5+}. Use of the formal–valence nomenclature B^{5+} merely indicates that the oxygen $2p$ bands are completely filled.

II. Size Considerations

The anion coordination about the A cation is determined primarily by the A-ion radius r_A. Empirically, it is found (*1*) that size considerations alone would stabilize A cations in a 12-coordinated site if $r_A > 0.9$ Å, in a six-coordinated (octahedral) site if $r_A < 0.8$ Å, so long as $r_B < 0.7$ Å. [The ionic radii are those of Shannon and Prewitt (*2*)]. Of the various A^+ ions, only the Li^+ ion ($r_{Li} = 0.74$ Å) is small enough to be normally stabilized in an octahedral (or lesser-coordinated) interstice of an oxygen array. All the others are large enough to be readily accommodated in a 12-coordinated site.

From the pioneering work of Katz and Ward and their associates at the University of Connecticut, a series of ABX_3 perovskite polytypes, containing 12-coordinated A cations, have been identified (*3*). These have been shown to form a regular family as a function of the relative ionic sizes (*4*). The several structures consist of ordered, close-packed AX_3 layers stacked in cubic (c) or hexagonal (h) or mixed cubic and hexagonal sequences, the smaller B cations occupying all the interlayer anion (X) octahedra. The various structures are identified by their particular stacking sequence. According to conventional polytype notation, they are referred to by the number of layers in a unit stacking sequence and by the symmetry of the primitive unit cell. Thus entirely cubic stacking is referred to as the 3C structure of cubic perovskite, and entirely hexagonal stacking as the 2H structure of $CsNiF_3$, see Fig. 1. These structures require not only that the B cation be stable in an octahedral interstice,

---

* This work was sponsored by the Department of the Air Force.

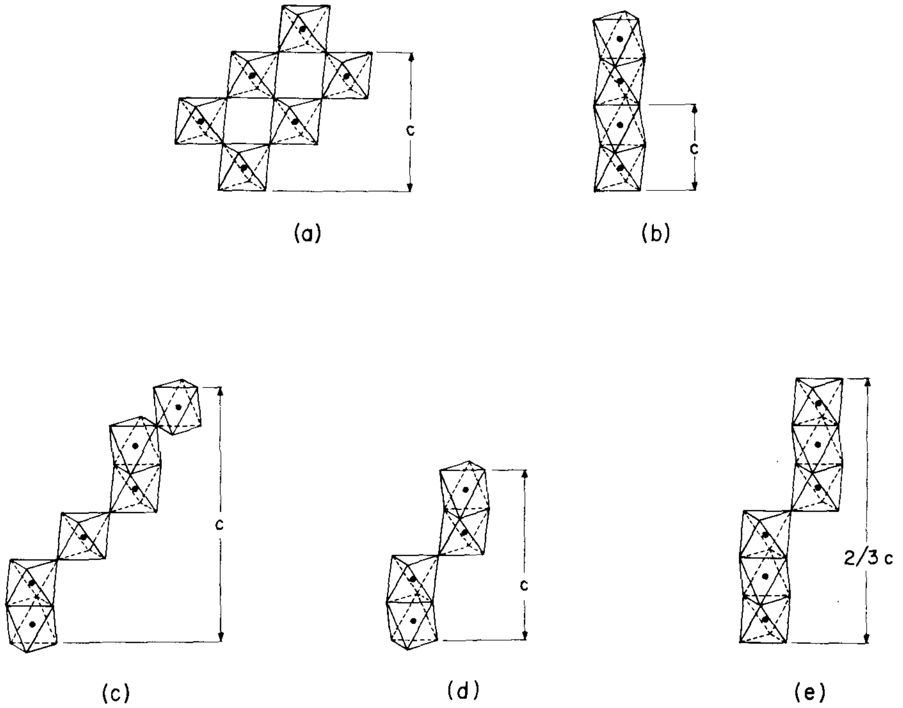

FIG. 1. Network of BX_6 octahedra in ABX_3 perovskite polytypes: (a) 3*C*, (b) 2*H*, (c) 6*H*, (d) 4*H*, and (e) 9*R*.

but also that the larger *A* cation have a radius r_A that is large enough to be compatible with AX_3 close-packed layers ($r_A > 0.9$ Å in oxides and fluorides).

In the 3*C* structure of Fig. 1(a), the *B*-cation octahedra share only corners, and the *A* cations are confined to a cubic cage of edge *B–X–B*. The *B–X* bond length is characteristic of the *B* and *X* ions, and considerable energy is required to increase it. Therefore, this cage creates an upper limit on the *A*-cation size that can be accommodated in a given BX_3 cubic array. This geometrical reasoning led Goldschmidt (*5*) to define a tolerance factor

$$t = (r_A + r_X)/\sqrt{2}(r_B + r_X) \qquad [1]$$

such that the ideal cubic structure should occur at $t = 1.0$. In the 2*H* structure of Fig. 1(b), on the other hand, the *B*-cation octahedra form face-shared linear chains parallel to the *c* axis. Since these chains are isolated from one another, relatively large *A* cations can be accommodated by adjustment of the *c*/*a* ratio. Therefore, this hexagonal structure is competitive for $t > 1$. Empirically, in a narrow transitional interval Δt there is a progression with *t* to phases having a greater proportion of hexagonal stacking: Fig. 1(c) has the two-to-one cubic-to-hexagonal stacking *cchcch* of hexagonal $BaTiO_{3-\delta}$–6*H*, Fig. 1(d) the *chch* stacking of hexagonal $SrMnO_3$–4*H*, and Fig. 1(e) the *chhchhchh* stacking of rhombohedral $BaRuO_3$–9*R*. The existence of these intermediate phases depends upon forces other than those due to ionic size alone.

III. Electrostatic Forces

A. Large A-Cations

The electrostatic forces between ions carrying an effective charge make a dominant contribution to the binding energies of polar crystals. This electrostatic binding energy is known as the Madelung energy.

Octahedral-site *B* cations suffer the largest mutual repulsive force if their octahedra share common faces, the smallest repulsive force if they are isolated, and intermediate repulsive forces if they share common corners or edges. Therefore, comparison of Figs. 1(a) and (b) shows that accommodation of a larger *A* cation ($t > 1$) in the 2*H* structure is accomplished at the expense of considerable Madelung energy. The relative importance of this loss in electrostatic binding energy depends upon the effective charge at the B cation and the spatial distribution of its outer electrons.

The electrostatic repulsive force between B cations in face-shared octahedra is reduced if only pairs—or at most triples—of B cations share faces, as illustrated by the three intermediate structures of Fig. 1. In this case opposite displacements along the c axis of the two B cations of a pair—or at the two ends of a triple—is accompanied by a cooperative contraction of the bridging anions, so a considerable enhancement of the Madelung energy can be achieved at the expense of relatively little elastic energy—provided t is not too much greater than unity. Nevertheless, the large effective charge on a B^{5+} ion can be expected to make face-shared octahedra—and hence the hexagonal polytypes—relatively unstable unless an aspherical distribution of outer-electron charge in B-cation d orbitals provides some B–B bonding.

B. Small A Cations

If both A and B cations occupy octahedral sites, the electrostatic Madelung energy would stabilize a close-packed anion array and an ordering of A and B cations that minimizes the electrostatic repulsive forces. Whether cubic or hexagonal, close packing of the anions produces close-packed planes of edge-shared octahedra and one octahedral interstice per anion. For a composition ABO_3, one out of three octahedral sites in these planes is empty, and Fig. 2 illustrates the ordering—of vacancies and of A and B cations of different effective charge—within these planes that minimizes the electrostatic repulsive forces between cations. Cubic stacking of these planes introduces six additional edge-shared sites per cation in adjacent planes, four of which are occupied, whereas hexagonal stacking introduces two face-shared sites per cation, only one of which need be occupied. Therefore, electrostatic forces would stabilize hexagonal stacking of the close-packed anion layers.

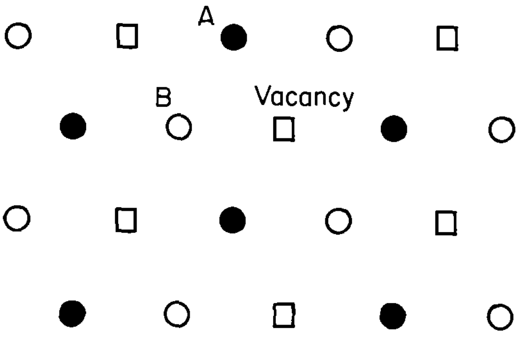

FIG. 2. Ordering within close-packed planes of anion octahedra that would optimize the electrostatic Madelung energy, given different effective charges or octahedral-site A and B cations of an ABO_3 compound.

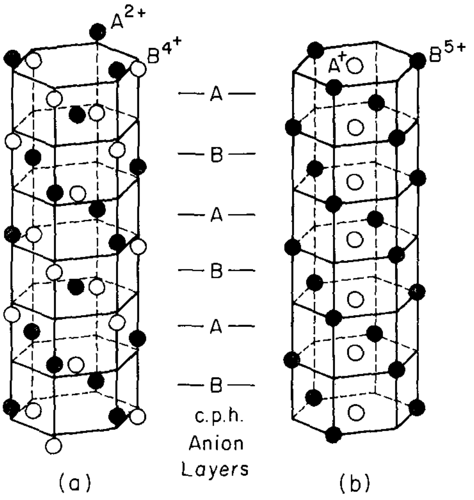

FIG. 3. Cation ordering in octahedral sites of a close-packed hexagonal-anion array that would optimize the electrostatic Madelung energy, given octahedral-site cations and compositions (a) $A^{2+}B^{4+}O_3$, (b) $A^+B^{5+}O_3$.

The cation ordering in successive close-packed layers would, according to electrostatic arguments, depend upon the effective charges at the cations. An $A^{2+}B^{4+}O_3$ composition, for example, would optimize the electrostatic forces by a pairing of an A and a B cation in face-shared octahedra, as illustrated in Fig. 3(a), whereas $A^+B^{5+}O_3$ compositions would superpose A^+ ions and alternate the B^{5+}-ion occupancy in successive basal planes as shown in Fig. 3(b). In Fig. 3(a), the electrostatic repulsive forces between cations can be further reduced by cation displacements parallel to the c axis away from the shared octahedral-site face. A cooperative contraction of the triangle of bridging anions minimizes the associated loss in elastic energy.

IV. Covalent Bonding

A. A–O Bonding

In the $A^+B^{5+}O_3$ compositions, the covalent contribution to the A–O bond is relatively weak. Nevertheless it provides a perturbation energy that is strong enough to distort the ideal structures arrived at from size and electrostatic considerations. For example, A–O bonding may distort the $3C$ structure of Fig. 1(a) from cubic to lower symmetry, particularly if the tolerance factor is $t < 1$ or if the A cation has a relatively unstable core, as in the case $A^+ = Tl^+$, Cu^+, or Ag^+ with $6s^2$, $3d^{10}$, and $4d^{10}$ cores, respectively.

The alkali-metal A^+ cations all have stable cores, and in the presence of a $t < 1$ they may distort the $3C$ perovskite phase from cubic to the *Pbnm* symmetry of orthorhombic $GdFeO_3$ or to the $R\bar{3}c$ symmetry of $LaAlO_3$ (*1*).

The Tl^+ ion, like the Pb^{2+} and Bi^{3+} ions, has a polarizable $6s^2$ core. The core polarization is due to $6s6p$ hybridization, and s–p hybridization energies are relatively small. If the A–O binding energy to be gained is greater than the hybridization energy, then spontaneous core polarization may displace each A cation cooperatively from the center of symmetry of its interstice to form some shorter A–O bonds, as in $BiFeO_3$ (*6*). Ferroelectric $PbTiO_3$ has a tetragonal ($c/a > 1$) distortion of the $3C$ structure of Fig. 1(a) that manifests a spontaneous $6s^2$-core polarization cooperative with ferroelectric displacements of the Ti^{4+} ions (*1*). Several $Pb^{2+}B^{4+}O_3$ compounds crystallize in a defect-pyrochlore structure, space-group $Fd3m$, corresponding to $Pb_2B_2O_6\square$. The anion vacancy occupies the unique anion positions, which are coordinated by four Pb atoms, and stability of this structure relative to the $3C$ structure of Fig. 1(a) has been interpreted as another manifestation of spontaneous $6s^2$-core polarization (*7*).

Polarization of a d^{10} core is due to d–s hybridization. Since these wave functions are even, the nucleus remains at the center of the charge distribution. At a copper atom, core polarization generally manifests itself as an oxidation from Cu^+ to Cu^{2+} with the formation of square-coplanar Cu–X bonds. The Ag^+ ion is not so readily oxidized, and core polarization is expressed as a nonspherical charge distribution.

B. B–O *Bonding*

Covalent bonding of an anion to two near-neighbor cations is stronger if different anionic orbitals are used for each cation–anion bond. Covalent σ bonding on opposite sides of an anion requires a sharing of the same anionic p_σ orbital in two different B–O bonds. Therefore, covalent bonding of an anion to two near-neighbor cations is stronger if these cations are on the same side of the anion. However, the covalent binding energy to be gained is reduced if the cations contain empty d orbitals available for π bonding. As illustrated for Nb^{5+} and Ta^{5+} ions in Fig. 4, an anion p orbital that σ bonds with one cation π bonds with the other if the B–O–B angle is 90°. Therefore, the anion p orbitals share in covalent bonding with two cations whether the cations are on the same or on opposite sides of the anion, and the covalent-binding energy to be gained by having the two cations on the same side of the anion is reduced by the factor $(1 - f_{\pi\sigma})$, where $f_{\pi\sigma}$ is the ratio of the π-bond to σ-bond covalent-binding energies. The Sb^{5+} and Bi^{5+} ions have filled d^{10} cores, which do not participate in π bonding, whereas the Nb^{5+} and Ta^{5+} ions have empty d^0 shells that participate strongly in covalent bonding with nearest-neighbor anions. Therefore, the covalent contribution to B–O bonding inhibits 180° B–O–B angles more strongly for the Sb^{5+} and Bi^{5+} ions.

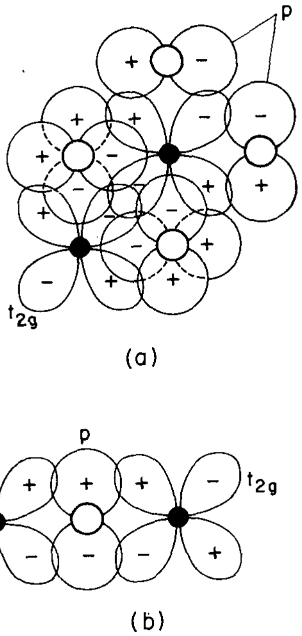

FIG. 4. Anion p and transition-metal-cation t_{2g} orbitals active in π bonding: (a) 90° B–O–B angles and (b) 180° B–O–B angles.

Another aspect of B–O bonding is the associated change in the spatial distribution of the bonding electrons. Charge transfer associated with σ-bonding electrons not only reduces the effective charges on the ions, but also distributes electronic charge along the bond axis. Charge transfer into π-bonding t_{2g} orbitals of a transition-metal cation, on the other hand, distributes electronic charge into the space between B–O bonds; and cations making a 90° B–O–B angle would concentrate the transferred charge along the B–B axis, where the crystalline fields create a deep electron potential. Blasse (*8*) has argued that this distribution of transferred π-bond charge creates a metal–metal bonding that can stabilize edge-shared—and even face-shared—octahedra containing Nb^{5+} or Ta^{5+} ions. Therefore, the electrostatic inhibitions of face-shared octahedra is smaller for Nb^{5+} and Ta^{5+} ions than for Sb^{5+} and Bi^{5+} ions. Although the increase in covalency associated with 90° vs 180° B–O–B angles tends to stabilize edge-shared octahedra containing Sb^{5+} or Bi^{5+} ions, no additional covalent energy is to be gained and considerable Madelung energy can be lost by forming face-shared octahedra with these ions.

In general, the stronger the B–X bonding, the greater the energy required to alter a B–X bond length. Moreover, as the size of the B cation is reduced relative to that of the anion, a critical size is reached where the stabilities of octahedral-site and tetrahedral-site coordination are about equal. Cations having an ionic radius close to the critical size may be stabilized in either octahedral or tetrahedral coordination, and the energy required to displace them from the center of symmetry of an octahedral site so as to reduce their coordination may be small even though the B–X bonding is strong. Furthermore, whether a crystal will exhibit a spontaneous displacement of the cation depends upon how other crystalline forces constrain the B–X bond length. If the B–X bond is stretched, a displacement may be induced. In oxides, transition-metal atoms from the beginning of a long period form ions with empty d shells (Ti^{4+}; Zr^{4+}; Hf^{4+}, Ta^{5+}) that tend to be stabilized in octahedral sites, whereas heavier atoms of a long period form ions with empty d shells (V^{5+}, Cr^{6+}; Mo^{6+}; Re^{7+}) that tend to be stabilized in tetrahedral sites. The intermediate ions Nb^{5+} and W^{6+} appear to be readily stabilized in both. Therefore, it is not surprising that ferroelectric-type displacements are generally associated with octahedral-site V^{5+}, Mo^{6+} and W^{6+} ions, and in more special cases with Ti^{4+} and Nb^{5+} ions (*1*). These distortions may be enhanced by cooperative core polarizations at the A cations, as occurs in $PbTiO_3$.

V. $A^+B^{5+}O_3$ Structures

The structures observed for the $A^+B^{5+}O_3$ compounds having B = Nb, Ta, Sb, or Bi are summarized in Table I. The tolerance factors t are indicated in parentheses. It is immediately apparent that the Nb^{5+} and Ta^{5+} ions are found in structures that are quite different from those stabilized by Sb^{5+} and Bi^{5+} ions. This fact should reflect the influence of π bonding at the Nb^{5+} and Ta^{5+} ions, since the four B cations are similar in all other respects.

Significantly, none of the $Li^+B^{5+}O_3$ oxides crystallize in either of the structures illustrated in Fig. 3. Superficially, $LiNbO_3$ and $LiTaO_3$ exhibit the order of Fig. 3(a), as might be expected for a B-cation charge considerably reduced from the formal–valence value. However, the structure in fact shows no displacement of the B cations along the c axis, only a displacement of each Li^+ ion to the far face of its interstice, which is midway between successive B^{5+} ions along the c axis (see Fig. 5(a)). Small, cooperative displacements of the Li^+ ions from this anion plane are responsible for the ferroelectric properties of $LiNbO_3$ and $LiTaO_3$ (*9*). Face-shared pairs of Nb^{5+} or Ta^{5+}, which are found in $Mg_4Nb_2O_9$ and $Mg_4Ta_2O_9$ (*10*), do not form in $LiNbO_3$ and $LiTaO_3$. Thus B–O bonding is here manifest by a stabilization of the B^{5+} ion in the center of an octahedral interstice. This stabilization is at the expense of a smaller anion coordination for the Li^+ ion. Similar structures were found for $CuNbO_3$ and $CuTaO_3$ prepared at 65 kbar, although the $CuNbO_3$ structure is distorted to monoclinic symmetry (*11*). The origin of this distortion was not determined. At atmospheric pressure, the Cu^+ ion of $CuTaO_3$ is oxidized to Cu^{2+} so that the stable phase is $Cu_{0.5}TaO_3$. The cations occupy the cation positions of the 3C structure, the Cu^{2+} ions being distributed on A sites. The TaO_3 array consists of corner-shared octahedra, as in the 3C structure, but the octahedra are buckled in such a way that each Cu^{2+} ion has four coplanar anion nearest neighbors that nearly form a square (*12*, *13*). This structure is apparently stabilized by a spontaneous deformation of the A-cation core that is enhanced by oxidation from a $3d^{10}$ to a $3d^9$ configuration. In the high-pressure phase $CuTaO_3$, accommodation of the relatively large Cu^+ ion in an octahedral-site face seems to require deformation of the $3d^{10}$ core without oxidation.

The influence of B–O bonding is illustrated more strikingly in $LiSbO_3$. Although this compound has one-third of its c-axis chains filled with Li^+ ions and the remaining two-thirds half-filled with Sb^{5+} ions ordered into alternate sites along

TABLE I

TOLERANCE FACTORS (t) AND STRUCTURES[a] OF SEVERAL $A^+B^{5+}O_3$ COMPOSITIONS. PRESSURE P IN KBAR

A	B			
	Nb	Ta	Sb	Bi
Li	(0.74) $R3c$	(0.74) $R3c$	(0.75) $Pncn$ $Im3)^b$	
Na	(0.94) $Pbnm$	(0.94) $Pbnm$	(0.96) $R\bar{3}$ $Im3)^b$	(0.90) $R\bar{3}$ $Im3)^f$
K	(1.04) $Amm2 \xrightarrow{225^\circ} \text{tet } 3C \xrightarrow{435^\circ} 3C$	(1.04) $3C$	(1.05) $R\bar{3} \xrightarrow{1000^\circ} Pn3$ $Im3$ at $P > 20$	(0.99) $Im3)^f$
Rb	(1.085) $Amm2$ at $P > 65$	(1.085) $3C$ at $P > 90$	(1.09) $Pn3$, $Im3$ at $P > 20^c$	
Tl	(1.08) $Fd3m$		(1.09) Dist. $Pn3$ at $P > 20$	
Cu	(0.82) Mono.^{d} at $P = 65$	(0.82) $R3c$ at $P = 65$		
Ag	(0.94) Mono.$^e \xrightarrow{550^\circ} 3C$	(0.94) Mono.$^e \xrightarrow{485^\circ} 3C$	(0.98) $Fd3m$ $Im3$ at $P > 90$; $Im3)^b$	(0.90) $Im3)^b$

[a] $R3c$ (fig. 5a); $Pncn$ (Fig. 5b); $Im3$ and $Pn3$ (Fig. 6); $3C$ = cubic perovskite; $Pbnm$ = orthorhombic perovskite of $GdFeO_3$; $Amm2$ = orthorhombic perovskite of ferroelectric $BaTiO_3$; $R\bar{3}$ = ilmenite; $Fd3m$ = defect pyroclore.

[b] Metastable form prepared by ion exchange.

[c] $Pn3$ may form in interval $20 < P < 80$.

[d] Distorted $R3c$.

[e] Distorted $3C$ reflecting Ag^+-ion displacements.

[f] Stabilized by incorporation of H_2O.

the c axis, as predicted in Fig. 3(b), nevertheless within each basal plane, the Sb^{5+} ions are not ordered as predicted in Fig. 2, but as shown in Fig. 5(b) (*14*). The zig-zag strings of edge-shared octahedra, which reduce the symmetry of the $LiSbO_3$ structure from hexagonal to orthorhombic, clearly demonstrate that some energy term other than ionic size and the electrostatic Madelung energy is playing a major role in determining the crystal structure. This term can only arise from covalent bonding, which is much more important in the B–O than in the A–O bonds. Each anion has two B-cation and two A-cation near neighbors; and the covalent-binding energy is maximized by having the two B cations on the same side of the anion, forming a 90° or a 109° B–O–B angle. This is particularly true of the Sb^{5+} or Bi^{5+} ions, which have no d orbitals available for π bonding. Therefore, stabilization of the cation ordering of Fig. 5(b) relative to that of Fig. 2 can be interpreted as a demonstration that the covalent-binding energy gained by forming ca. 90° B–O–B angles is larger than the electrostatic energy that is lost. The stability of this phase relative to the $LiNbO_3$ structure can then be attributed to the stability of 90° vs 135° Sb–O–Sb bonds. For Nb^{5+} and Ta^{5+} ions, a relatively large $f_{\pi\sigma}$ reduces the importance of this energy term.

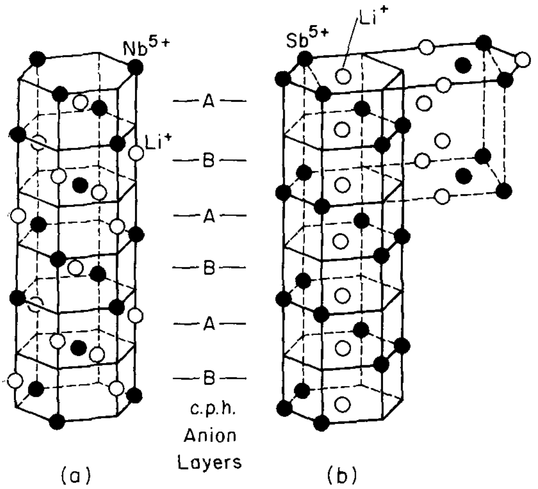

FIG. 5. Cation ordering found in octahedral sites of a close-packed anion array for (a) $LiNbO_3$ and $LiTaO_3$, (b) $LiSbO_3$.

The importance of B–O covalent-binding energy is already manifest in the titanates $M^{2+}Ti^{4+}O_3$ that crystallize in the ilmenite structure, which has space group $R\bar{3}$. In this structure, cations occupy the same octahedral sites as indicated in Fig. 3(a), but there is no ordering of M^{2+} and Ti^{4+} ions within basal planes as illustrated in Fig. 2. Rather, alternate basal planes of cations are all M^{2+} or all Ti^{4+} ions. Clearly, ordering of the A and B cations within basal planes has been sacrificed in order to place two Ti^{4+} ions on the same side of each anion, making ca. 90° B–O–B angles.

Crystallization of $NaSbO_3$ and $KSbO_3$ in the ilmenite ($R\bar{3}$) structure rather than the orthorhombic (*Pbnm*) or cubic (3*C*) perovskite structure provides another example of the formation of ca. 90° B–O–B angles in preference to 180° B–O–B angles. The Na^+ and K^+ ions, which are normally too large for an octahedral site, stabilize the niobates and tantalates in perovskite 3*C* structures at high temperatures. At lower temperatures, the sodium compounds, having $t < 1$, are distorted to orthorhombic (*Pbnm*) symmetry by Na–O bonding. The ca. 180° B–O–B angles can be stabilized because of the large π-bond contribution to the covalent bonding of Nb^{5+} and Ta^{5+} ions. Where π bonding is absent, the covalent contribution to the binding energy does not permit stabilization of 180° B–O–B angles.

Spiegelberg (*15*) has reported that $KSbO_3$, after annealing for several weeks at 1000°C, transforms to a cubic phase—either primitive cubic (*Pn*3) or body-centered cubic (*Im*3) (*13*). We have found that high pressures stabilize the *Im*3 structure, and Hong (*13*) has shown that an isostructural $NaSbO_3$ phase—metastable at room temperature—can be prepared from either cubic form of $KSbO_3$ by ion exchange. Each cubic phase contains the $Sb_{12}O_{36}$ network of Fig. 6. This network is built up of pairs of edge-shared octahedra —Sb_2O_6 units—that have common corners, and each anion has two Sb^{5+} near neighbors on the same side making B–O–B angles α in the range $90° < \alpha < 135°$. A similar $Bi_{12}O_{36}$ network is stabilized by H_2O in $NaBiO_3$ and $KBiO_3$ (*16*). The stability of this network relative to the BO_3 network of the 3*C* structure of Fig. 1(a) provides clear evidence that B–O covalent bonding plays an important role in structure stabilization, a role that does not manifest itself in $NaNbO_3$, $NaTaO_3$, $KNbO_3$ and $KTaO_3$ because of the presence of strong π bonding.

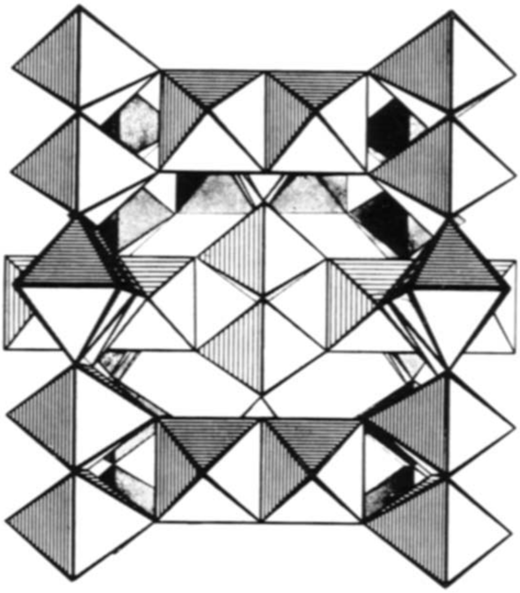

FIG. 6. The $Sb_{12}O_{36}$ network found in *Pn*3 and *Im*3 structures of $KSbO_3$.

The $B_{12}O_{36}$ network of Fig. 6 contains tunnels of face-shared octahedra along the ⟨111⟩ directions that intersect at the origin and body-center positions. The successive octahedral-site faces along a half-diagonal of the unit cell consist of O_1 and O_2 triangles in the sequences O_1–O_2–O_2–O_1, and the area of the O_2 triangles is smaller than that of the O_1 triangles. In the *Pn*3 structure, the A^+ ions are ordered. In four tetrahedral directions from the origin, A^+ ions occupy the two O_1–O_2 octahedra; and in the other four directions, they occupy the O_2–O_2 octahedron. In the *Im*3 structure, the Na^+ and K^+ ions are randomly distributed over the octahedral sites whereas the small Li^+ and polarizable Ag^+ ions appear to occupy randomly the centers of the O_2 triangles (*13*).

It is reasonable to ask why the K^+BO_3 compounds, all of which have a $t > 1$, do not crystallize in one of the hexagonal polytypes of Fig. 1. Indeed, in the 2*H* structure of Fig. 1(b), all of the anions have two near-neighbor cations making a ca. 90° B–O–B bond angle. Therefore, why isn't this structure competitive even for $KSbO_3$ and $KBiO_3$? The answer seems to be that B^{5+}–B^{5+} repulsive forces are too strong for face-shared octahedra to be stable. In the ilmenite phase a B^{5+} and an A^+ ion share common faces, and in the $B_{12}O_{36}$ network of Fig. 6 the B^{5+} ions share edges. Although this conclusion is anticipated for Sb^{5+}

and Bi^{5+} ions, it is somewhat surprising for the Nb^{5+} and Ta^{5+} ions in view of the cation ordering found in $Mg_4Nb_2O_9$ and $Mg_4Ta_2O_9$. It suggests that π bonding is strong enough to stabilize face-shared pairs only if these pairs are isolated. It would therefore be interesting to know whether the composition $Ba_3Nb_2MgO_9$ can be prepared in the $6H$ structure.

The formation of $3C$ perovskites in compositions having $t > 1$ indicates that stretching of the B–O bonds costs less energy than formation of face-shared octahedra. In the titanates and niobates, stretching of the B–O bonds induces a ferroelectric displacement of the B cations—$BaTiO_3$ ($t = 1.06$) and $KNbO_3$ ($t = 1.04$) are ferroelectric whereas $CaTiO_3$ ($t = 0.97$) and $NaNbO_3$ ($t = 0.94$) are not. On the other hand, no stretching of the B–O bonds is required for WO_3 and MoO_3 to exhibit anti-ferroelectric transitions, and stretching of the B–O bond in $KTaO_3$ ($t = 1.04$) does not induce a ferroelectric transition. These observations suggest the criterion $d > d_c$ for ferroelectric distortions of ABO_3 compounds having the $3C$ perovskite structure, where d is the B–O bond length and d_c is its critical value for tetrahedral vs octahedral site preference. It appears that $d \lesssim d_c$ for $A^{2+}Ti^{4+}O_3$ and $A^{+}Nb^{5+}O_3$ compounds having $t < 1$, but that $d > d_c$ can be satisfied by a stretching of the B–O bond. In the $A^{+}TaO_3$ compounds, $d < d_c$ remains even after stretching of the B–O bond, whereas $d \gtrsim d_c$ in MoO_3 and WO_3 even without any stretching.

In order to test further this hypothesis, it was decided to prepare $RbNbO_3$ and $RbTaO_3$, which have a $t = 1.085$. These phases have not been prepared (at least as perovskites) at atmospheric pressure, presumably because the tolerance factor requires too large a stretching of the B–O bond for the $3C$ phase to be stable while the B^{5+}–B^{5+} electrostatic repulsion is too large for an hexagonal polytype to be stable. However, previous studies (*17*) have shown that pressure decreases t, since the A–O bonds are more compressible than the B–O bonds, and therefore the $3C$ phase should be stabilized by high pressure. Furthermore, such high-pressure phases are generally metastable at room temperature and atmospheric pressure. As can be seen from Table I, both $RbNbO_3$ and $RbTaO_3$ were successfully prepared above 65 and 95 kbar, respectively (*18*). Like $KNbO_3$ and $KTaO_3$, at room temperature $RbNbO_3$ exhibits the ferroelectric distortion of orthorhombic $BaTiO_3$ whereas $RbTaO_3$ is cubic. Both $RbNbO_3$ and $RbTaO_3$ disproportionate on heating without transforming to a hexagonal polytype. Therefore, we may conclude that electrostatic forces prevent formation of the hexagonal polytypes in $A^{+}B^{5+}O_3$ compounds.

The existence of $TlNbO_3$ with the defect-pyrochlore structure ($Tl_2Nb_2O_6\square$) is consistent with the occurrence of this phase in several $PbB^{4+}O_3$ compounds, since Tl^{+} and Pb^{2+} ions both have polarizable $6s^2$ cores. In this structure, the B–O–B angles are ca. 130°, which makes it also a possible alternative for $A^{+}SbO_3$ and $A^{+}BiO_3$ compounds having a polarizable A^{+}-ion core. Indeed, in $AgSbO_3$—where the Ag^{+} ion has a polarizable $4d^{10}$ core—this structure is competitive at atmospheric pressure with the cubic $Pn3$ or $Im3$ structures. Pressure stabilizes the $Im3$ phase. The peculiar distortion from cubic symmetry in $AgNbO_3$ and $AgTaO_3$, which have $t < 1$, is due to a cooperative displacement of the Ag^{+} ions. This displacement, like the position of the Ag^{+} ion in the $Im3$ phase of $AgSbO_3$, is further evidence that the $4d^{10}$ core of an Ag^{+} ion may be spontaneously polarized.

VI. Final Comments

The ideas presented here are similar to those expressed by Blasse (*8*). However, Blasse focused his attention on the Nb^{5+}–Nb^{5+} and Ta^{5+}–Ta^{5+} bonding due to π-bond covalency. In addition to expanding these ideas, we have found that Sb^{5+} and Bi^{5+} ions, which do not pair in face-shared octahedra, have a much stronger preference energy for edge-shared 90° vs corner-shared 180° B–O–B angles.

The compounds $Ba_3Ru_2^{5+}M^{2+}O_9$, $M =$ Mg or Ni, crystallize in the $6H$ structure of Fig. 1(c), the M^{2+} ions ordering into the corner-sharing octahedra (*19*). The Ru^{5+} ions have two half-filled $4d$ orbitals available for Ru–Ru bonding, which may account for the stability of face-shared octahedra.

Sleight and Ward (*20*) and Blasse (*21*) have reported several $A_2^{2+}B^{3+}Sb^{5+}O_6$ cubic perovskites. In these compounds, ordering of the B cations doubles the cell of the $3C$ structure, so that each anion has only one Sb^{5+} near neighbor. In this case, covalent bonding is optimized by the formation of isolated SbO_6 complexes. Formation of the $3C$ structure is inhibited only where it requires the formation of 180° Sb^{5+}–O–Sb^{5+} bonds.

References

1. J. B. Goodenough and J. M. Longo, "Landolt–Bornstein Tabellen", p. 126, New Series III/4a, Springer–Verlag, Berlin (1970).
2. R. D. Shannon and C. T. Prewitt, *Acta Crystallogr.* **B25**, 925 (1969).
3. L. Katz and R. Ward, *Inorg. Chem.* **3**, 205 (1964); J. G. Dickinson, L. Katz, and R. Ward, *J. Am. Chem. Soc.* **83**, 3026 (1961); P. C. Donahue, L. Katz, and R. Ward, *Inorg. Chem.* **4**, 306 (1965) and **5**, 335 (1966).
4. J. M. Longo and J. A. Kafalas, *J. Solid State Chem.* **1**, 103 (1969).
5. V. M. Goldschmidt, *Akad. Oslo I. Mat.-Natur* **2**, 7 (1926).
6. C. Michel, J. M. Moreau, G. D. Achenbach, R. Gerson, and W. J. James, *Solid State Commun.* **7**, 701 (1969).
7. J. M. Longo, P. M. Raccah, and J. B. Goodenough, *Mater. Res. Bull.* **4**, 191 (1969).
8. G. Blasse, *J. Inorg. Nucl. Chem.* **26**, 1191 (1964).
9. P. Bailey, Thesis, University of Bristol, 1952.
10. E. F. Bertaut, L. Corliss, F. Forrat, R. Aléonard, and R. Pauthenet, *J. Phys. Chem. Solids* **21**, 234 (1961).
11. A. W. Sleight and C. T. Prewitt, *Mater. Res. Bull.* **5**, 207 (1970).
12. D. Reinen and V. Propach, *Inorg. Nucl. Chem. Lett.* **7**, 569 (1971).
13. H. Y-P. Hong, *Lincoln Laboratory Solid State Research Report* **2**, May 10, 1972.
14. M. Edstrand and N. Ingri, *Acta Chem. Scand.* **8**, 1021 (1954).
15. P. Spiegelberg, *Ark. Kemi. Mineral. Geol.* **14A**, No. 5, 1 (1940).
16. B. Aurivillius, *Acta Chem. Scand.* **8**, 1021 (1954); J. Zemann, *Mineral. Petrog. Mitt.* **1**, 361 (1950).
17. J. B. Goodenough, J. A. Kafalas, and J. M. Longo, *in* "Preparative Methods in Solid State Chemistry" (P. Hagenmuller, Ed.), Chap. 1, Academic Press (1972).
18. J. A. Kafalas, "Solid State Chemistry, Proc. 5th Materials Res. Symp." (R. S. Roth and S. J. Schneider, Eds.), N.B.S. Special Publication 364, July 1972.
19. A. Callaghan, C. W. Moeller, and R. Ward, *Inorg. Chem.* **5**, 1572 (1966).
20. A. W. Sleight and R. Ward, *Inorg. Chem.* **3**, 292 (1964).
21. G. Blasse, *J. Inorg. Nucl. Chem.* **27**, 993 (1965).